ELSEVIER

Chemical Engineering Journal 127 (2007) 167–176

Chemical Engineering Journal

www.elsevier.com/locate/cej

Photocatalytic degradation of an azo dye in a tubular continuous-flow photoreactor with immobilized TiO_2 on glass plates

M.A. Behnajady [a,*], N. Modirshahla [a], N. Daneshvar [b], M. Rabbani [c]

[a] *Research Laboratory, Department of Applied Chemistry, Islamic Azad University, Tabriz Branch, P.O. Box 1655, Tabriz, Islamic Republic of Iran*

[b] *Water and Wastewater Treatment Research Laboratory, Department of Applied Chemistry, Faculty of Chemistry, University of Tabriz, C.P. 51664 Tabriz, Islamic Republic of Iran*

[c] *Department of Applied Chemistry, Faculty of Chemistry, Islamic Azad University, North Tehran Branch, P.O. Box 19585/936, Tehran, Islamic Republic of Iran*

Received 28 February 2006; received in revised form 3 September 2006; accepted 16 September 2006

Abstract

The photocatalytic degradation of C.I. Acid Red 27 (AR27), an anionic monoazo dye of acid class, in aqueous solutions was investigated in a tubular continuous-flow photoreactor with immobilized TiO_2 on glass plates. The removal percent is a function of photoreactor length, volumetric flow rate and light intensity. The removal efficiency increases as the light intensity increases but it decreases when the flow rate is increased. The AR27 degradation was followed through HPLC, UV–vis and chemical oxygen demand (COD) analyses. The results of these analyses showed that the final outlet stream from the photoreactor was considerably mineralized. NH_4^+, NO_3^-, NO_2^- and SO_4^{2-} ions were analyzed as mineralization products of nitrogen and sulfur heteroatoms, respectively. Results show that the final concentration of SO_4^{2-} ions and N-containing mineralization products are less than the final expected stoichiometric values. Based on the results obtained in present and previous studies, a reaction pathway for the photocatalytic degradation of AR27 is proposed. The kinetic analysis of the decolorization of AR27 in continuous-mode shows a pseudo-first-order reaction. Results show that a linear relation exists between pseudo-first-order reaction rate constant and reciprocal of volumetric flow rate.

Keywords: Advanced oxidation processes (AOPs); UV/TiO_2; Heterogeneous photocatalysis; Decolorization; Continuous-flow photoreactor; C.I. Acid Red 27

1. Introduction

Dyes and pigments are important industrial chemicals and play an important role in the textile industry [1]. The number of dyes presently used in textile industry is about 10,000. Among these dyes, azo dyes constitute the largest and the most important class of commercial dyes [2]. The release of these dyes into the environment causes severe ecological problems. The textile wastewaters have strong color and high chemical oxygen demand (COD). In addition, azo dyes and their derived products are known to present serious carcinogenic effect [1]. For the treatment of these dyes biological process is ineffective. Also common treatment processes, e.g. adsorption on activated carbon, flocculation and electrocoagulation [3] are not efficient methods because they merely transfer dye from water to solid and, hence, produce secondary wastes. Therefore, it is necessary to develop destructive systems leading to complete mineralization of these dyes.

Recent developments in the domain of chemical water treatment gave birth to an improvement of the oxidative and catalytic degradation of organic compounds dissolved in aqueous media [4–10]. They are generally referred to as advanced oxidation processes (AOPs). The AOPs are able to breakdown many organic pollutants so that cheaper biological processes can be used as a second stage to achieve complete mineralization. This domain is particularly oriented towards application and has a strong impact on design and construction of new light sources, photochemical reactors, and the preparation of new photocatalysts and their supports [11]. Among the AOPs, photocatalysis system which is a combination of a semiconductor such as TiO_2-P25 (Degussa), TiO_2 (Merck), TiO_2-Hombikat UV-100 (Sachtleben Chemie GmbH), TiO_2-PC500 (Millennium Inorganic Chemicals), anatase TiO_2-BDH (BDH Corp.), ZnO, ZnS, Fe_2O_3, CdS, WO_3, ZrO_2, SrO_2, CeO_2, etc., with UV light is a very promising technique. TiO_2-P25 (Degussa) is extensively used as a standard active component for photocatalytic reactions. It is non-toxic

* Corresponding author. Tel.: +98 411 3320198; fax: +98 411 3313922.
E-mail address: behnajady@iaut.ac.ir (M.A. Behnajady).

1385-8947/$ – see front matter © 2006 Elsevier B.V. All rights reserved.
doi:10.1016/j.cej.2006.09.013

and has low price and due to a fast electron transfer to molecular oxygen, is found to be very efficient for photocatalytic degradation of pollutants [12–14]. It has been well demonstrated that when TiO_2 is illuminated by light ($\lambda < 390$ nm) electrons are promoted from the valence band to the conduction band to give electron–hole pairs. The holes at the TiO_2 valence band, having an oxidation potential of +2.6 V versus normal hydrogen electrode (NHE) at pH 7, can oxidize water or hydroxide to produce hydroxyl radicals. The hydroxyl radical is a powerful oxidizing agent and attacks to organic compounds, under favorable conditions, the final products being H_2O, CO_2 and inorganic anions [11].

The development of UV/TiO_2 process in order to achieve complete mineralization of organic pollutants has been widely tested for a large variety of chemicals [11]. Since photocatalysts are often applied in the form of suspension or slurry [4,8,15], from application point of view it is practically difficult due to problems of separation of the nanoparticles of TiO_2 and the recycling of the photocatalyst. In the slurry systems, the catalyst must be removed with a solid–liquid separation stage which adds to the overall capital and running costs of the plant [16]. In order to make the environmental application of TiO_2 photocatalysis more practical, immobilization of TiO_2 on a certain substrate is required. TiO_2-P25 (Degussa) can be immobilized onto a solid substrate such as sand, polymer films and glass [17–19]. Unfortunately little attention has been diverted to design continuous-flow photoreactors with immobilized TiO_2 on a solid surface [20–23].

In the present work, we described the construction and performance of a continuous-flow photoreactor with immobilized TiO_2 on glass plates for decolorization and mineralization of C.I. Acid Red 27 as a model compound from anionic monoazo dye of acid class.

2. Experimental

2.1. Materials

AR27, a monoazo anionic dye, was obtained from Boyakh Saz Company (Iran). Its chemical structure is given in Fig. 1. Titanium dioxide was Degussa P-25 and it constitutes approximately 80% anatase and 20% rutile. It had a BET surface area of $50 \pm 15\ m^2\ g^{-1}$ and an average particle diameter of 21 nm, containing 99.5% TiO_2.

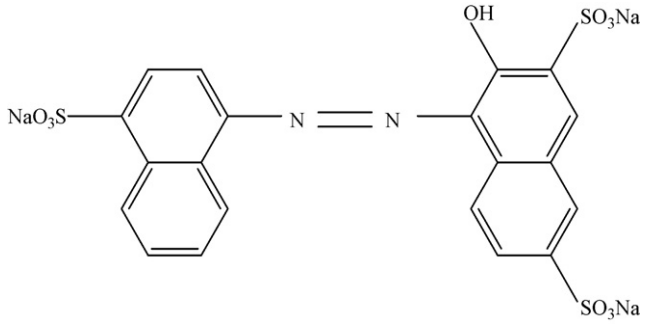

Fig. 1. Chemical structure of AR27 (C.I. 16185).

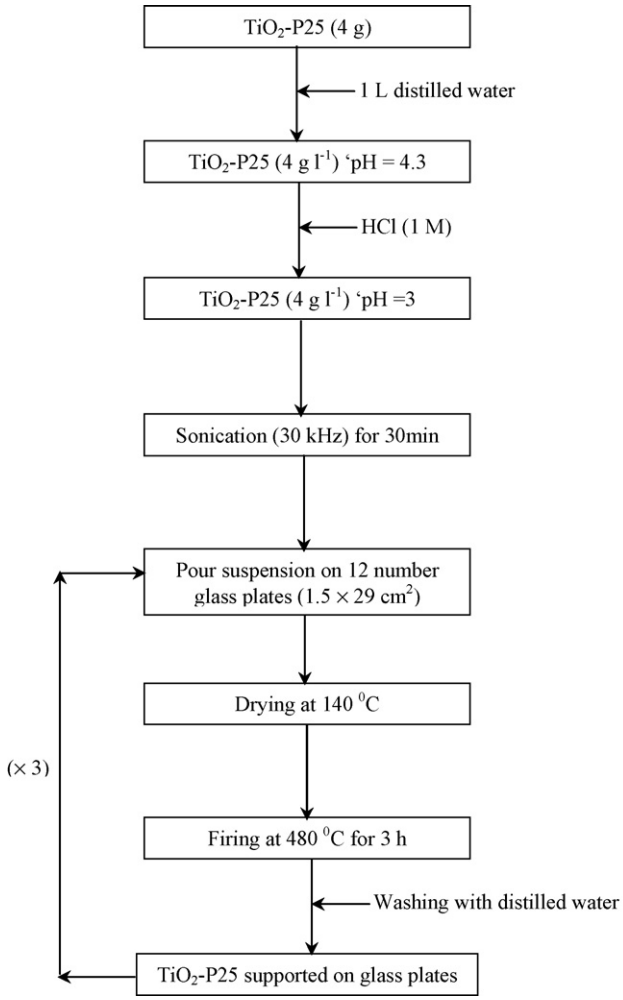

Scheme 1. Schematic diagram of the heat attachment method for immobilizationof TiO_2-P25 on glass plates.

2.2. Immobilization of TiO_2-P25 on glass plates

To prepare the immobilized TiO_2-P25 on glass plates (1.5 cm × 29 cm) heat attachment method was used [19]. In this procedure, a suspension containing 4 g l^{-1} TiO_2-P25 in distilled water was prepared. Then, the pH was adjusted to about 3 by HCl (1 M). Prepared suspension was sonicated in an ultrasonic bath (T460H, Windaus) under frequency of 30 kHz for 30 min in order to improve the dispersion of TiO_2-P25 in water. Glass plates treated with a dilute HF solution and washed in a solution of NaOH (0.01 M) in order to increase the number of OH groups and better contact of TiO_2-P25 on glass plates. In this stage, sonicated suspension was poured on 12 glass plates and then placed in an oven at 140 °C. After drying, the glass plates were fired at 480 °C for 3 h and washed with distilled water for the removal of weakly attached TiO_2-P25 particles. Deposition process was carried out four times to increase the loaded TiO_2-P25 on the surface of the glass plates (Scheme 1). Fig. 2 shows scanning electron microscope (SEM) picture of TiO_2-P25 which is immobilized on the glass plates.

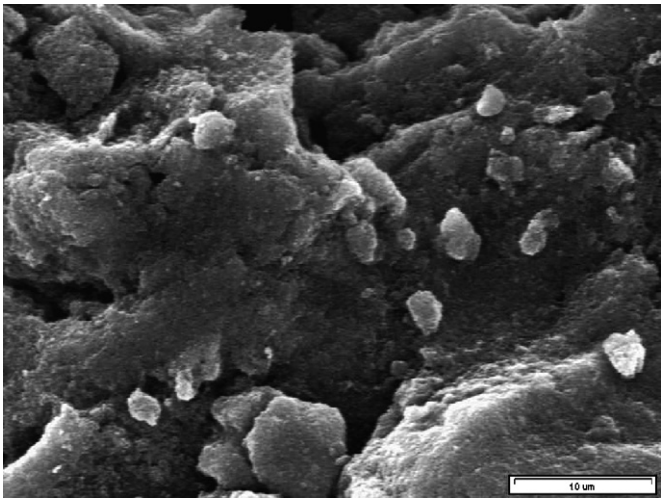

Fig. 2. SEM micrograph of TiO_2-P25 immobilized on glass plate.

2.3. Photoreactor

All experiments were carried out in a tubular continuous-flow photoreactor, which has been shown in Fig. 3. The photoreactor comprises four quartz tubes (24.4 mm i.d., 26 mm o.d.), which were serially connected by means of transparent polyethylene tubes from the top to the bottom. Three glass plates loaded with TiO_2-P25 was inserted in each quartz tubes. The radiation sources were four low pressure mercury UV lamps (30 W, UV-C, λ_{max} = 254 nm, manufactured by Philips, Holland), which were placed in front of the quartz tubes. The light sources emit UV in the 200–300 nm range or that portion of the UV spectrum called UV-C. Ninety-five percent of the relative intensity occurs at the mercury discharge line of 254 nm. Changing the distance between the lamps and the quartz tubes would vary the light intensity.

2.4. Procedures

For photocatalytic degradation of AR27, a solution containing known concentration of AR27 was prepared and then 2 l of the prepared solution was transferred into a Pyrex beaker and agitated with a magnetic stirrer during experiment. For saturation of solution with oxygen, it was continuously purged with O_2 through a gas disperser placed at the bottom of the Pyrex beaker before and during the illumination. The solution was pumped with a peristaltic pump (Heidolph, PD 5001) through the irradiated quartz tubes, and AR27 concentration at the inlet and outlet was analyzed with a UV–vis spectrophotometer (Ultrospec 2000, Biotech Pharmacia, England) at 521 and 254 nm. The absorbance at 521 nm is due to the color of the dye solution and it is used to monitor the decolorization of the dye. The absorbance at 254 nm represents the aromatic content of AR27 and absorbance decrease at 254 nm indicates the degradation of aromatic part of the dye [24–26]. The degree of decolorization and degradation as a function of time is given by:

$$\text{Decolorization}\,(\%) = \frac{A_0\,(521\,\text{nm}) - A\,(521\,\text{nm})}{A_0\,(521\,\text{nm})} \times 100 \quad (1)$$

$$\text{Degradation}\,(\%) = \frac{A_0\,(254\,\text{nm}) - A\,(254\,\text{nm})}{A_0\,(254\,\text{nm})} \times 100 \quad (2)$$

where A_0 is the initial absorbance of AR27 and A represents the absorbance of AR27 at time t for corresponding wavelengths.

The changes in the absorption spectra of AR27 at different lengths of photoreactor were recorded on a double-beam UV–vis spectrophotometer (Shimadzu 1700) in the wavelength range from 190 to 700 nm.

The formation of SO_4^{2-}, NH_4^+, NO_3^- and NO_2^- ions were determined by turbidimetric, direct nesslerization and spectrophotometric methods, respectively [27]. Chemical oxygen demand was measured by the dichromate reflux method [28].

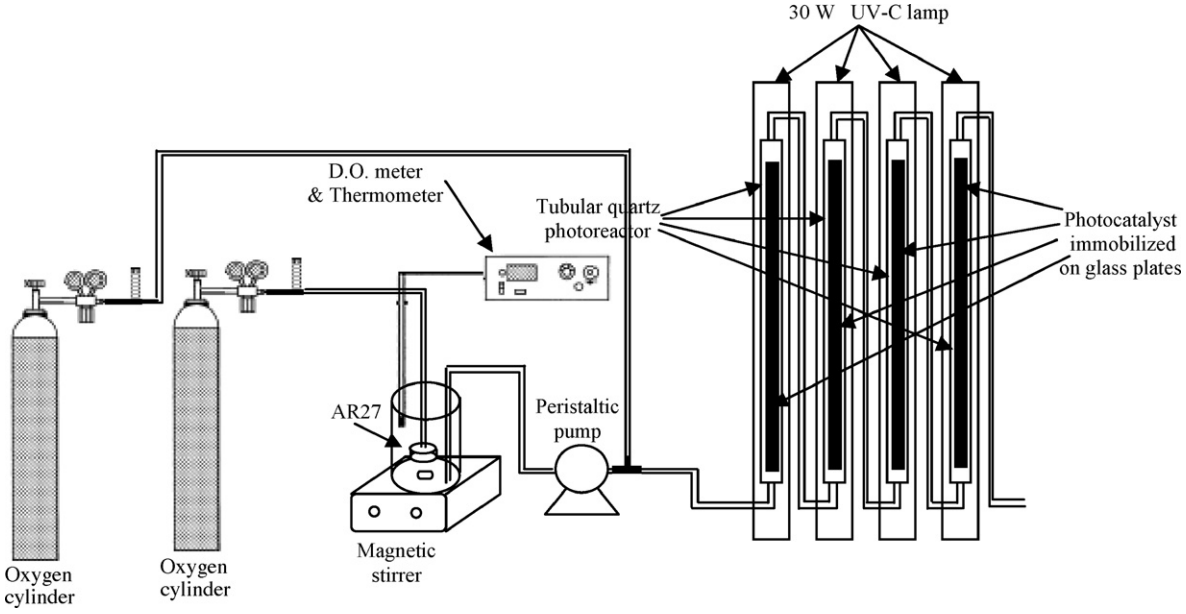

Fig. 3. Schematic diagram of tubular continuous-flow photoreactor. For details, refer to the text.

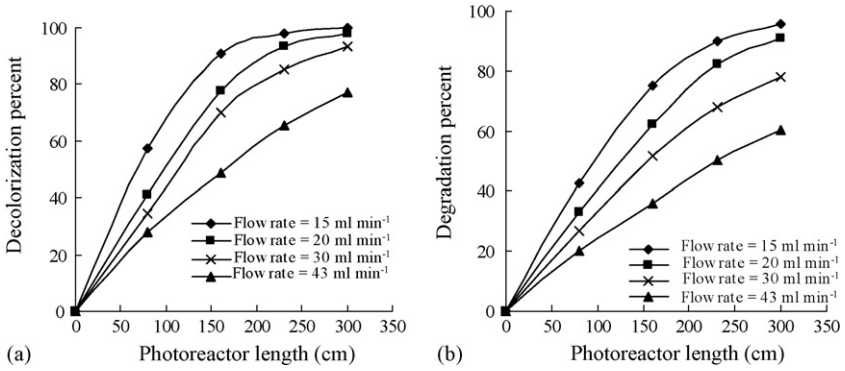

Fig. 4. Effect of the flow rate at decolorization (a) and degradation (b) of AR27 in UV/TiO_2 process at continuous-mode. $[AR27]_0 = 30\,mg\,l^{-1}$; $I_0 = 58\,W\,m^{-2}$.

High-performance liquid chromatograms were recorded on an HPLC (Perkin-Elmer Series 200). A Spheri-5 RP-18 column with dimension of 220 mm × 4.6 mm and with 5 μm particle size and UV–vis detector with the wavelength set at 254 nm were used. The mobile phase was a mixture of acetonitrile–water 30/70 (v/v) at a flow rate of 0.9 ml min^{-1}.

The light intensity in the center of the photoreactor was measured by a Lux-UV-IR meter (Leybold Co., GmbH). The SEM picture of immobilized TiO_2-P25 on glass plates was recorded with SEM Cambridge S360.

3. Results and discussion

3.1. The effect of flow rate

The decolorization and degradation efficiency versus photoreactor length at different flow rates have been summarized in Fig. 4a and b, respectively. The results indicate that with decreasing flow rate from 43 to 15 ml min^{-1}, removal efficiency is increased, so that the complete decolorization and degradation was obtained at around 230 and 310 cm of photoreactor length, respectively. This is logical, because with decreasing flow rate the residence time of the reactant increases in the reactor. Results in Fig. 4a and b show that the degradation of AR27 aromatic content is rather slower than decolorization. This can be attributed to the formation of intermediates, resulting from the photocatalytic degradation of AR27, which still contains aromatic rings. This trend was observed by other researchers, such as Mahmoodi et al. [25] showed the degradation of Direct Red 80 in a TiO_2 fixed bed reactor was slower than decolorization of this compound.

3.2. The effect of light intensity

The effect of the light intensity at the decolorization and degradation of AR27 was shown in Fig. 5. The results show that the removal percent steadily increases with increasing the light intensity linearly. The increase in the light intensity from 18.8 to 58.5 W m^{-2} increases the decolorization from 25 to 42% and degradation from 13 to 28% for 80 cm of photoreactor length. The results show that the UV light intensity plays an important role in degradation of AR27. Previous studies indicated that at low light intensities, the reaction rate would increase linearly with increasing light intensity (first order), at intermediate light intensities the reaction rate would depend on the square root of the light intensity (half order), and at high light intensities the reaction rate was independent of the light intensity [29]. These results appear that the UV light intensities employed in this study lie within the linear range. Decolorization of AR27 in the absence of UV-light ($I_0 = 0\,W\,m^{-2}$) as a result of adsorbtion of AR27 on TiO_2 surface in reaction condition was very small and it can be neglected. This result is in agreement with findings of Mahmoodi et al. [30] at photocatalytic degradation of C.I. Acid Red 14 on TiO_2.

3.3. Mineralization and final degradation products of AR27

Mineralization of AR27 in this process was studied by COD loss, changes in HPLC chromatograms and UV–vis spectra and also SO_4^{2-}, NH_4^+, NO_3^- and NO_2^- evolution at different lengths of photoreactor.

COD values have been related to the total concentration of organics in the solution and the decrease of COD reflects the degree of mineralization as a function of photoreactor length. Fig. 6 shows the decrease of COD versus photoreactor length, as it appears final COD value in outlet stream of photoreactor is very low. These results show that outlet stream from photoreactor is considerably mineralized. The persistence of a constant level of COD in final stream suggests that the accumulated of

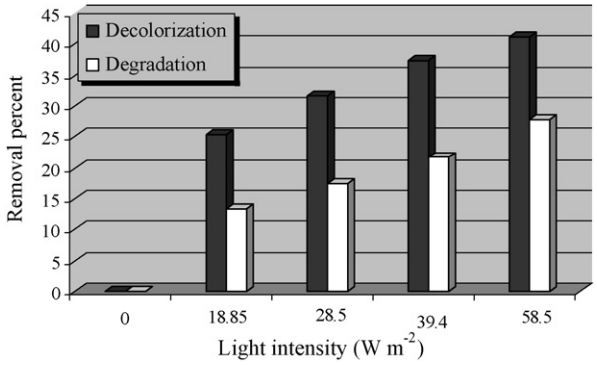

Fig. 5. Effect of the light intensity at degradation and decolorization of AR27. $[AR27]_0 = 30\,mg\,l^{-1}$; flow rate = 20 ml min^{-1}; photoreactor length = 80 cm.

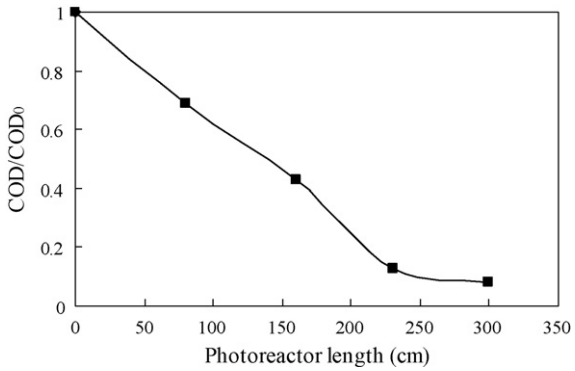

Fig. 6. COD changes vs. photoreactor length. $[AR27]_0 = 30\,mg\,l^{-1}$; flow rate = 10 ml min^{-1}; $I_0 = 58\,W\,m^{-2}$.

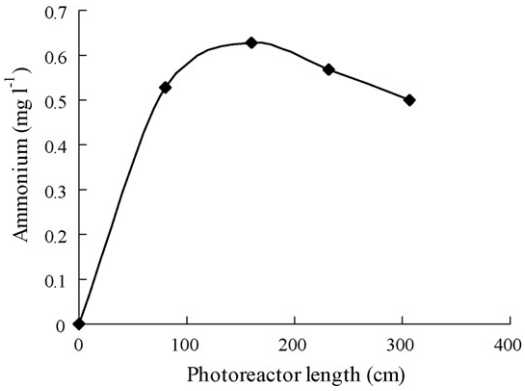

Fig. 8. NH_4^+ evolution vs. photoreactor length. For details, refer to Fig. 7.

dead-end products are resistant to degradation by the UV/TiO_2 process.

The evolution of SO_4^{2-} ions is presented in Fig. 7 versus photoreactor length. According to the AR27 molecular structure in Fig. 1, three sulfonic groups attached into two kinds of naphthalene rings. Fig. 7 shows the initial amount of SO_4^{2-} ions is very low for 80 cm of photoreactor length. This result indicates that SO_4^{2-} ions form after decolorization stage and breakdown of nitrogen-to-nitrogen double bond (–N=N–) of the azo dye. It is observed that the concentration of SO_4^{2-} ions continuously increases and reaches a plateau of 7.5 mg l^{-1} for 250 cm of photoreactor length. The concentration of SO_4^{2-} ions in outlet stream of photoreactor is less than the expected value for complete mineralization of the dye. This result shows that almost 48% of SO_4^{2-} ions are adsorbed on the photocatalyst surface [31].

The evolution of NH_4^+, NO_3^- and NO_2^- as N-containing mineralization products versus photoreactor length are given in Figs. 8 and 9. The nitrogen mass balance, obtained with considering NH_4^+, NO_3^- and NO_2^- concentrations, shows that the concentration of N-containing mineralization products is 3.3 times less than the final expected stoichiometric value. This could be explained by the formation of N_2, therefore almost 70% of N heteroatoms transforms to N_2 [32]. As can be seen from Figs. 8 and 9, the main N-containing mineralization product of photocatalytic degradation of AR27 is NH_4^+. Figs. 8 and 9 show the initial slope is positive for NH_4^+, NO_3^- and NO_2^- with no delay time like with SO_4^{2-}, indicating these ions are initial products, directly resulting from the initial attack on the nitrogen-to-nitrogen double bond (–N=N–) of the azo dye.

The changes in the UV–vis absorption spectra of AR27 solutions during the photocatalytic degradation process at different photoreactor lengths have been shown in Fig. 10. The decrease of the absorption peak of AR27 at λ = 521 nm in Fig. 10 indicates a rapid degradation of the azo dye. The decrease is also meaningful with respect to the nitrogen-to-nitrogen double bond (–N=N–) of the azo dye, as the most active site for oxidative attack. As can be seen from Fig. 10a, in the final outlet stream from photoreactor, absorption spectra in the UV–vis regions were not disappeared for flow rate of 44 ml min^{-1}. With decreasing the flow rate to 15 ml min^{-1} absorption spectrum in the UV–vis regions for final outlet stream of the photoreactor is considerably reduced (Fig. 10c). The decrease in the volumetric flow rate from 44 to 15 ml min^{-1} increases decolorization from 77.27 to 100% and degradation from 57.14 to 95.24%. These results are in good agreement with HPLC chromatograms (Fig. 11). The analysis of HPLC chromatograms of the solution at different photoreactor lengths revealed the formation of intermediate products at the retention time of 1.24 min. In the flow rate of 10 ml min^{-1}, intermediates and AR27 peaks for final outlet stream of the photoreactor are considerably reduced (Fig. 11).

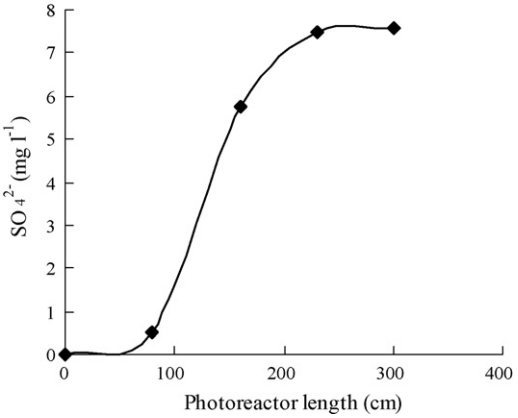

Fig. 7. SO_4^{2-} evolution vs. photoreactor length. $[AR27]_0 = 30\,mg\,l^{-1}$; flow rate = 10 ml min^{-1}; $I_0 = 58\,W\,m^{-2}$.

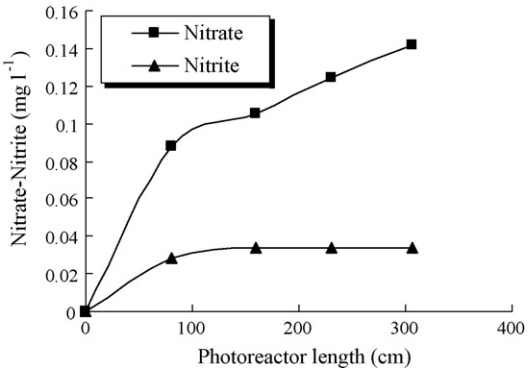

Fig. 9. NO_3^- and NO_2^- evolution vs. photoreactor length. For details, refer to Fig. 7.

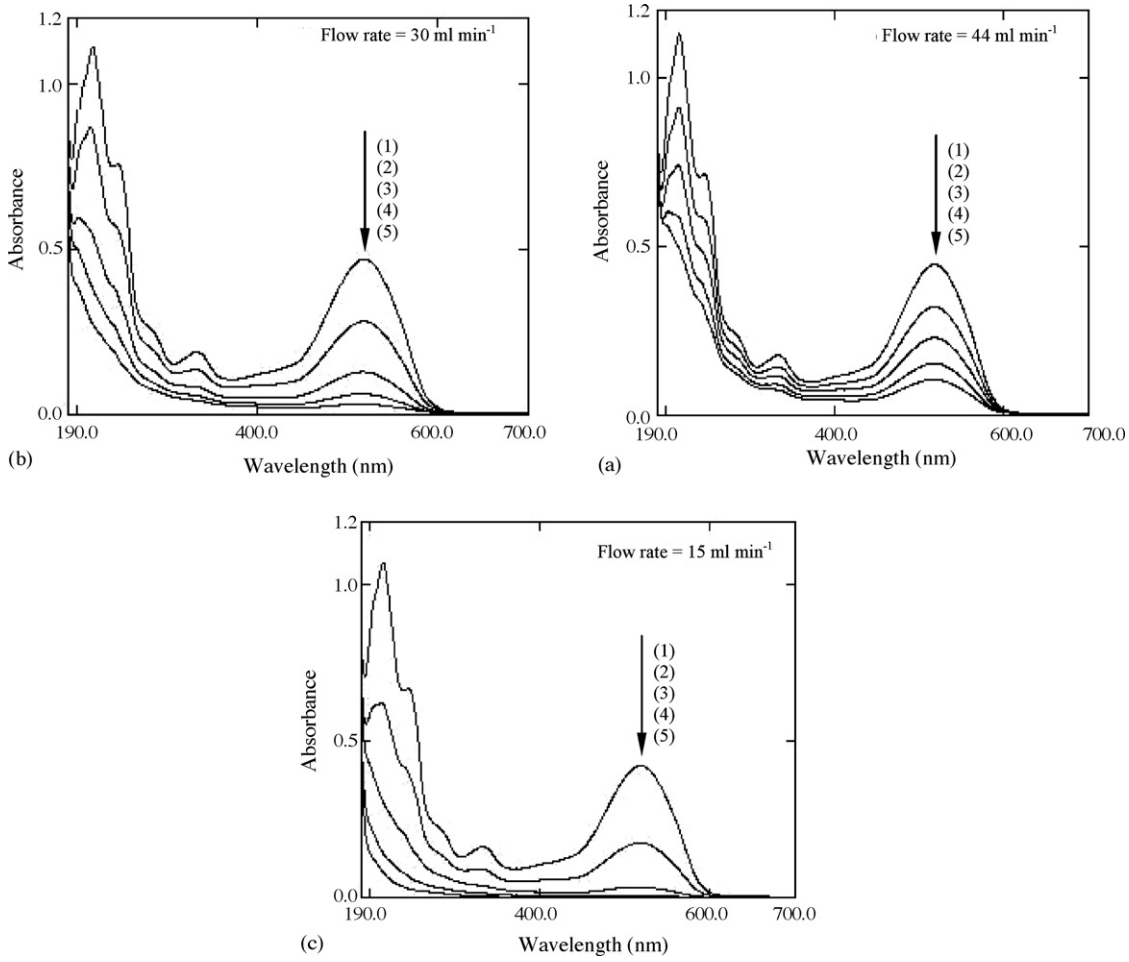

Fig. 10. UV–vis spectral changes of AR27, recorded during the dye degradation at different photoreactor lengths. (1) 0 cm, (2) 80 cm, (3) 160 cm, (4) 231 cm and (5) 300 cm. $[AR27]_0 = 30\ mg\ l^{-1}$; $I_0 = 58\ W\ m^{-2}$.

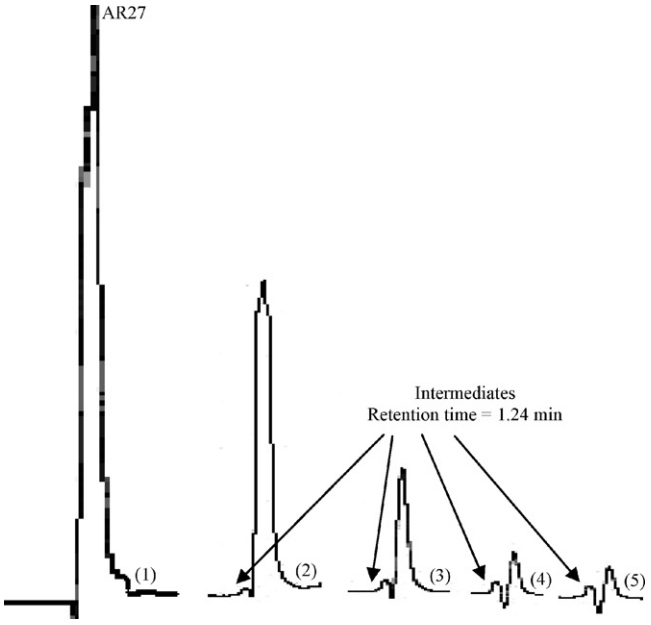

Fig. 11. HPLC chromatograms of the AR27, recorded during the dye degradation at different photoreactor lengths. (1) 0 cm, (2) 80 cm, (3) 160 cm, (4) 231 cm and (5) 300 cm. $[AR27]_0 = 30\ mg\ l^{-1}$; flow rate = 10 ml min^{-1}; $I_0 = 58\ W\ m^{-2}$.

3.4. The mechanism of AR27 degradation

AR27 solution comprises an azo and hydrazone mixture. AR27 is subjected to intermolecular hydrogen bonding tautomeric interactions between the oxygen of the naphtyl group and β-hydrogen of the corresponding of azo-linkage. Factors such as solvent, play a significant role in determining the tautomeric equilibrium. The ratio of the azo form to the hydrazone form is much higher in organic solvents than in water. The hydrazone form is usually more stable in water [33]. Based on the results obtained in this and previous studies [34,35], a reaction pathway for the photocatalytic degradation of AR27 is proposed, as schematically shown in Scheme 2. The positive slope of N-containing mineralization products and the lack for SO_4^{2-} ions evolution show that the first step most probably involves cleavage of the AR27 molecule at the level of the very active azo band. The rapid decrease of AR27 absorbance peak at 521 nm is evident for this trend, also transforming of N heteroatom to N_2 and other N-containing products show two different degradation pathways should be suggested. In first pathway, the reaction can be initiated by one-electron injection to AR27 hydrazone form. Oxidative cleavage of produced compound forms an unstable compound which rapidly produces N_2. Further oxidation

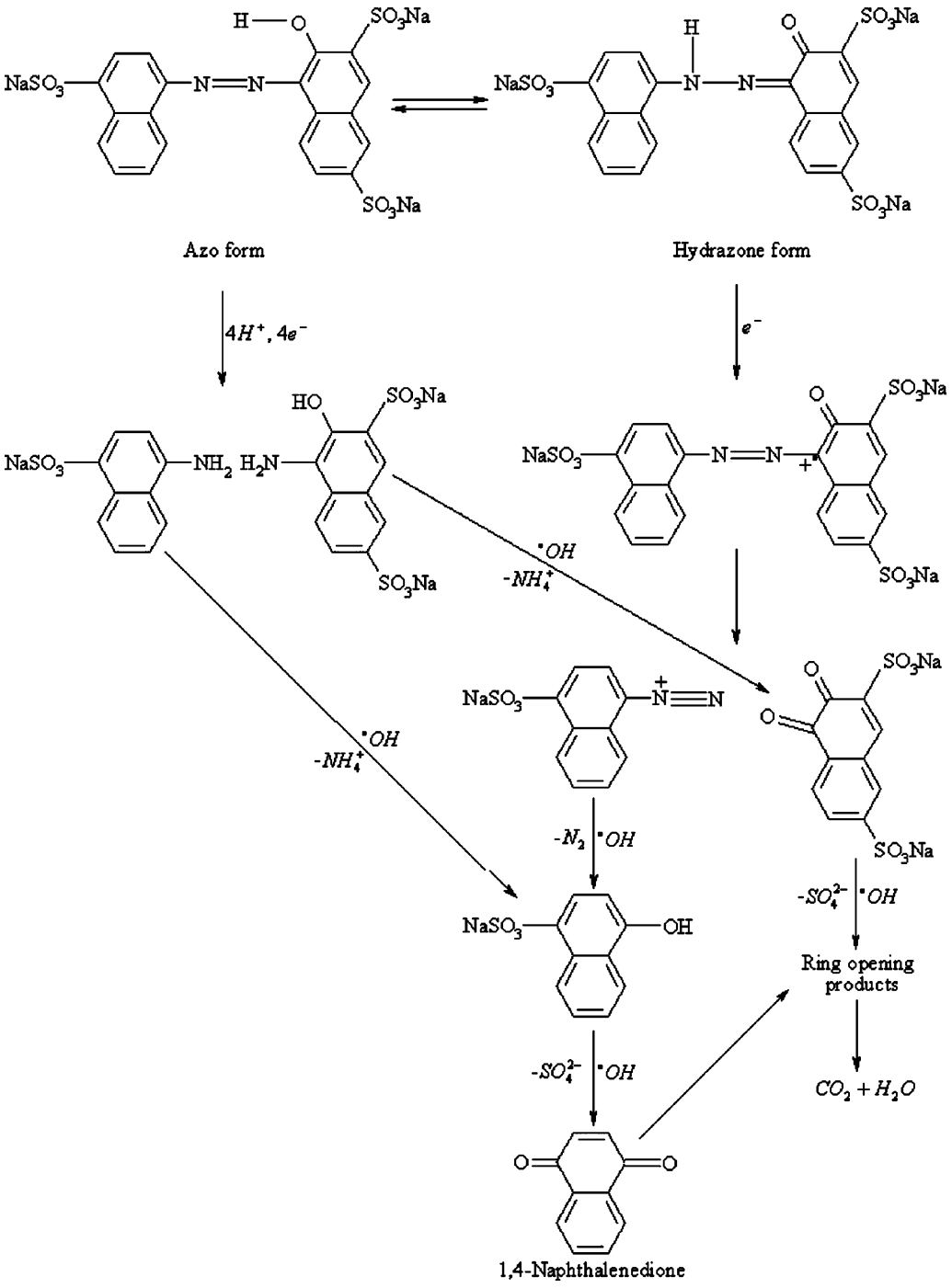

Scheme 2. Degradation mechanism of AR27 from two different pathways.

leads to SO_4^{2-} ions evolution and compounds containing a naphthalenic ring such as 1,4-naphthalenedione, which these compounds cleavage eventually to CO_2. Stylidi et al. [34] have identified 1,4-naphthalenedione and other compounds containing a naphthalenic ring during the photocatalytic degradation of C.I. Acid Orange 7 (a monoazo anionic dye from acid class). The release of SO_4^{2-} ions can be accounted as an initial attack by hydroxyl radicals according to:

$$R\text{–}SO_3^- + {}^\bullet OH \rightarrow R\text{–}OH + SO_3^{\bullet -} \quad (3)$$

$$SO_3^{\bullet -} + {}^-OH \rightarrow SO_4^{2-} + H^\bullet \quad (4)$$

The hydrogen atom $H^\bullet$ can subsequently react with hydroxyl radicals [32]:

$$H^\bullet + {}^\bullet OH \rightarrow H_2O \quad (5)$$

In the second pathway, AR27 might be reduced with injection of electrons to nitrogen-to-nitrogen double bond (–N=N–) of the azo form and decolorization occurs. The release of amino containing intermediates was detected with Bilgi and Demir [35]

at the photocatalytic degradation of C.I. Reactive Orange 16 (a monoazo anionic dye from acid class). The nitrogen atoms in the amino groups can be led to NH_4^+ and NO_3^- ions by successive attacks of hydroxyl radicals [36].

3.5. The kinetic analysis of AR27 decolorization in continuous-flow photoreactor

The photocatalytic oxidation kinetics of many organic compounds have often been modeled with the Langmuir–Hinshelwood equation. This model was developed by Turchi and Ollis [37] and expressed as Eq. (6):

$$R = -\frac{\mathrm{d[AR27]}}{\mathrm{d}t} = \frac{k_{\mathrm{L-H}} K_{\mathrm{ads}}[\mathrm{AR27}]}{1 + K_{\mathrm{ads}}[\mathrm{AR27}]} \tag{6}$$

where R is the reaction rate (mg l^{-1} min^{-1}), $k_{L–H}$ the reaction rate constant (mg l^{-1} min^{-1}), K_{ads} the adsorption coefficient of dye on the TiO_2 particles (mg^{-1} l), and [AR27] the concentration of dye (mg l^{-1}). Al-Ekabi and Serpone [38] have admitted that the rate should include competitive adsorption by intermediates. Under these reasonable conditions, Eq. (6) can be written as follows:

$$R = -\frac{\mathrm{d[AR27]}}{\mathrm{d}t} = \frac{k_{\mathrm{L-H}} K_{\mathrm{ads}}[\mathrm{AR27}]}{1 + K_{\mathrm{ads}}[\mathrm{AR27}] + \sum K_{\mathrm{i}} C_{\mathrm{i}}} \tag{7}$$

In this equation K_i and C_i are the adsorption equilibrium constant and concentration for intermediates, respectively. Beltran-Heredia et al. [39] made the following assumption:

$$K_{\mathrm{ads}}[\mathrm{AR27}] + \sum K_{\mathrm{i}} C_{\mathrm{i}} = K_{\mathrm{ads}}[\mathrm{AR27}]_0 \tag{8}$$

In this equation $[AR27]_0$ is the initial concentration of AR27. With substituting Eq. (8) in to Eq. (7), we obtain:

$$R = -\frac{\mathrm{d[AR27]}}{\mathrm{d}t} = \frac{k_{\mathrm{L-H}} K_{\mathrm{ads}}[\mathrm{AR27}]}{1 + K_{\mathrm{ads}}[\mathrm{AR27}]_0} = k_{\mathrm{ap}}[\mathrm{AR27}] \tag{9}$$

which

$$k_{\mathrm{ap}} = \frac{k_{\mathrm{L-H}} K_{\mathrm{ads}}}{1 + K_{\mathrm{ads}}[\mathrm{AR27}]_0} \tag{10}$$

Eq. (9) shows a pseudo-first-order reaction with respect to the AR27 concentration. The design equation for a plug-flow reactor (PFR) is [40]:

$$\frac{-\mathrm{d[AR27]}}{\mathrm{d}V} = \frac{-r_{\mathrm{AR27}}}{\nu_0} \tag{11}$$

with

$$V = \frac{\pi}{4} d_{\mathrm{i}}^2 l - V_{\mathrm{glass\ plate}} \tag{12}$$

and

$$V_{\mathrm{glass\ plate}} = abl \tag{13}$$

and

$$-r_{\mathrm{AR27}} = \frac{-\mathrm{d[AR27]}}{\mathrm{d}t} \tag{14}$$

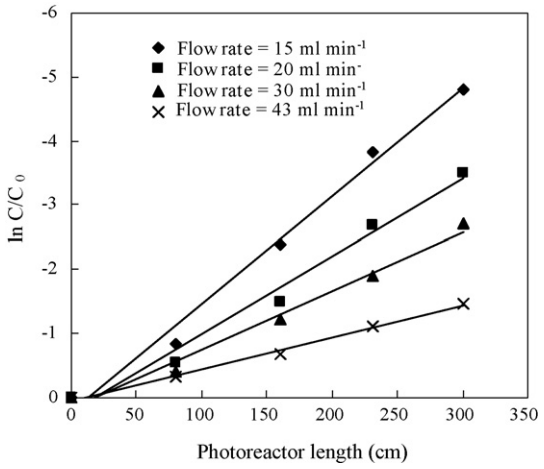

Fig. 12. Derivation of k'_{ap} for photocatalytic degradation of AR27 in the continuous-flow photoreactor in UV/TiO_2 process by linear regression. For details, refer to Fig. 4.

In the above equations V, ν_0, d_i, l, a and b are the photoreactor volume, volumetric flow rate, inner diameter of quartz tubular photoreactor, photoreactor length, depth and width of the glass plates, respectively. With substituting Eqs. (12)–(14) into Eq. (11), we obtain:

$$\frac{-\mathrm{d[AR27]}}{\mathrm{d}l} = \frac{(\pi/4)d_{\mathrm{i}}^2 - ab}{\nu_0} \left(\frac{-\mathrm{d[AR27]}}{\mathrm{d}t} \right) \tag{15}$$

Finally, with substituting of Eq. (9) into Eq. (15), we obtain:

$$\frac{-\mathrm{d[AR27]}}{\mathrm{d}l} = \frac{((\pi/4)d_{\mathrm{i}}^2 - ab)k_{\mathrm{ap}}}{\nu_0}[\mathrm{AR27}] \tag{16}$$

After integration of this equation for initial condition $[AR27] = [AR27]_0$ for $l = 0$ cm from photoreactor length, leads to:

$$\ln\frac{[\mathrm{AR27}]}{[\mathrm{AR27}]_0} = -\frac{((\pi/4)d_{\mathrm{i}}^2 - ab)k_{\mathrm{ap}}}{\nu_0} l = -k'_{\mathrm{ap}} l \tag{17}$$

which

$$k'_{\mathrm{ap}} = \frac{((\pi/4)d_{\mathrm{i}}^2 - ab)k_{\mathrm{ap}}}{\nu_0} \tag{18}$$

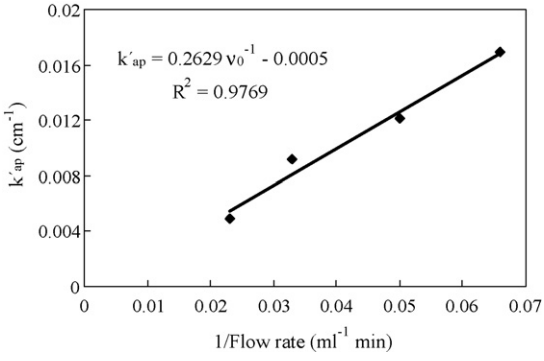

Fig. 13. Relation between k'_{ap} with volumetric flow rate. For details, refer to Fig. 4.

The semi-logarithmic graphs of the concentration of AR27 at different volumetric flow rates versus photoreactor lengths yield straight lines indicating pseudo-first-order reaction. The k'_{ap} for photocatalytic degradation of AR27 was evaluated from experimental data (Fig. 12) using a linear regression. As shown in Fig. 13 a linear relation exists between k'_{ap} and $1/\nu_0$, which is also in agreement with Eq. (18). These results indicate that with decreasing ν_0, as a result of enhancement of residence time the k'_{ap} values increase.

4. Conclusions

UV/TiO_2 process with immobilized photocatalyst on glass plates in continuous-mode can be used for complete degradation of AR27 as a model compound from monoazo anionic dyes. Removal efficiency of AR27 in this process increases linearly with increasing the light intensity. With decreasing flow rate, final COD was very low, also HPLC chromatograms and UV–vis absorption peaks mainly disappeared. The formation of NH_4^+, NO_3^- and NO_2^- ions at the beginning of the reaction and rapid decrease of absorption peak of AR27 at $\lambda_{max} = 521$ nm show that these ions are initial products directly resulting from the initial attack on the nitrogen-to-nitrogen double bond (–N=N–) of the azo dye. The formation of SO_4^{2-} ions at the beginning of the reaction is very low, which indicates that SO_4^{2-} ions form after decolorization stage. Transforming of N heteroatom to N_2 and other N-containing products show two different degradation pathways can be suggested for photocatalytic degradation of AR27. Kinetic analysis shows a pseudo-first-order reaction respect to AR27 concentration.

Acknowledgements

The authors thank the Islamic Azad University of Tabriz branch for financial and other supports, and also many thanks to Mrs. Skandari for HPLC chromatograms.

References

[1] K. Golka, S. Kopps, Z.W. Myslak, Carcinogenicity of azo colorants: influence of solubility and bioavailability, Toxicol. Lett. 151 (2004) 203–210.
[2] M. Neamtu, I. Siminiceanu, A. Yediler, A. Kettrup, Kinetics of decolorization and mineralization of reactive azo dyes in aqueous solution by the UV/H_2O_2 oxidation, Dyes Pigments 53 (2002) 93–99.
[3] N. Daneshvar, H. Ashassi-Sorkhabi, A. Tizpar, Decolorization of orange II by electrocoagulation method, Sep. Purif. Technol. 31 (2003) 153–162.
[4] N. Daneshvar, M. Rabbani, N. Modirshahla, M.A. Behnajady, Kinetic modeling of photocatalytic degradation of Acid Red 27 in UV/TiO_2 process, J. Photochem. Photobiol. A 168 (2004) 39–45.
[5] N. Daneshvar, M. Rabbani, N. Modirshahla, M.A. Behnajady, Critical effect of hydrogen peroxide concentration in photochemical oxidative degradation of C.I. Acid Red 27 (AR27), Chemosphere 56 (2004) 895–900.
[6] N. Daneshvar, M. Rabbani, N. Modirshahla, M.A. Behnajady, Photooxidative degradation of Acid Red 27 (AR27): modeling of reaction kinetic and influence of operational parameters, J. Environ. Sci. Health A 39 (2004) 2319–2332.
[7] M.A. Behnajady, N. Modirshahla, M. Shokri, Photodestruction of Acid Orange 7 (AO7) in aqueous solutions by UV/H_2O_2: influence of operational parameters, Chemosphere 55 (2004) 129–134.
[8] M.A. Behnajady, N. Modirshahla, R. Hamzavi, Kinetic study on photocatalytic degradation of C.I. Acid Yellow 23 by ZnO photocatalyst, J. Hazard. Mater. B 133 (2006) 226–232.
[9] M.A. Behnajady, N. Modirshahla, Kinetic modeling on photooxidative degradation of C.I. Acid Orange 7 in a tubular continuous-flow photoreactor, Chemosphere 62 (2006) 1543–1548.
[10] M.A. Behnajady, N. Modirshahla, Evaluation of electrical energy per order (EEO) with kinetic modeling on photooxidative degradation of C.I. Acid Orange 7 in a tubular continuous-flow photoreactor, Ind. Eng. Chem. Res. 45 (2006) 553–557.
[11] O. Legrini, E. Oliveros, A.M. Braun, Photochemical processes for water treatment, Chem. Rev. 93 (1993) 671–698.
[12] B. Neppolian, H.C. Choi, S. Sakthivel, B. Arabindo, V. Murugesan, Solar/UV-induced photocatalytic degradation of three commercial textile dyes, J. Hazard. Mater. B 89 (2002) 303–317.
[13] M. Saquib, M. Muneer, TiO_2-mediated photocatalytic degradation of a triphenylmethane dye (gentian violet), in aqueous suspensions, Dyes Pigments 56 (2003) 37–49.
[14] C.C. Wong, W. Chu, The direct photolysis and photocatalytic degradation of alachlor at different TiO_2 and UV sources, Chemosphere 50 (2003) 981–987.
[15] N. Daneshvar, D. Salari, M.A. Behnajady, Decomposition of anionic sodium dodecylbenzene sulfonate by UV/TiO_2 and UV/H_2O_2 processes: a comparison of reaction rates, Iran. J. Chem. Chem. Eng. 21 (2002) 55–62.
[16] J.A. Byrne, B.R. Eggins, N.M.D. Brown, B. McKinney, M. Rouse, Immobilisation of TiO_2 powder for the treatment of polluted water, Appl. Catal. B 17 (1998) 25–36.
[17] R.W. Matthews, Photooxidative degradation of coloured organics in water using supported catalysts. TiO_2 on sand, Water Res. 25 (1991) 1169–1176.
[18] M.R. Dhananjeyan, J. Kiwi, K.R. Thampi, Photocatalytic performance of TiO_2 and Fe_2O_3 immobilized on derivatized polymer films for mineralization of pollutants, Chem. Commun. (2000) 1443–1444.
[19] S. Sakthivel, M.V. Shankar, M. Palanichamy, B. Arabindoo, V. Murugesan, Photocatalytic decomposition of leather dye: comparative study of TiO_2 supported on alumina and glass beads, J. Photochem. Photobiol. A 148 (2002) 153–159.
[20] M. Trillas, J. Peral, X. Domenech, Photocatalyzed degradation of phenol, 2, 4-dichlorophenol, phenoxyacetic acid and 2,4-dichlorophenoxyacetic acid over supported TiO_2 in a flow system, J. Chem. Tech. Biotechnol. 67 (1996) 237–242.
[21] K. Kobayakawa, C. Sato, Y. Sato, A. Fujishima, Continuous-flow photoreactor packed with titanium dioxide immobilized on large silica gel beads to decompose oxalic acid in excess water, J. Photochem. Photobiol. A 118 (1998) 65–69.
[22] G.R.R.A. Kumara, F.M. Sultanbawa, V.P.S. Perera, I.R.M. Kottegoda, K. Tennakone, Continuous flow photochemical reactor for solar decontamination of water using immobilized TiO_2, Solar Energy Mater. Solar Cells 58 (1999) 167–171.
[23] M.J. Garcia-Martinez, L. Canoira, G. Blazquez, I. Da Riva, R. Alcantara, J.F. Llamas, Continuous photodegradation of naphthalene in water catalyzed by TiO_2 supported on glass Raschig rings, Chem. Eng. J. 110 (2005) 123–128.
[24] M. Muruganandham, M. Swaminathan, Photochemical oxidation of reactive azo dye with $UV–H_2O_2$ process, Dyes Pigments 62 (2004) 271–277.
[25] N.M. Mahmoodi, M. Arami, N.Y. Limaee, N.S. Tabrizi, Decolorization and aromatic ring degradation kinetics of Direct Red 80 by UV oxidation in the presence of hydrogen peroxide utilizing TiO_2 as a photocatalyst, Chem. Eng. J. 112 (2005) 191–196.
[26] M. Stylidi, D.I. Kondarides, X.E. Verykios, Pathways of solar light-induced photocatalytic degradation of azo dyes in aqueous TiO_2 suspensions, Appl. Catal. B 40 (2003) 271–286.
[27] ASTM, Annual Book of ASTM Standards, Water and Environmental Technology, vol. 11.01, Philadelphia, PA, 2000.
[28] APHA/AWWA/WPCF, Standards Methods for the Examination of Water and Wastewater, 17th ed., American Public Health Association, Washington, DC, 1989.
[29] R. Terzian, N. Serpone, Heterogeneous photocatalyzed oxidation of creosote components: mineralization of xylenols by illuminated TiO_2 in

oxygenated aqueous media, J. Photochem. Photobiol. A 89 (1995) 163–175.
[30] N.M. Mahmoodi, M. Arami, Bulk phase degradation of Acid Red 14 by nanophotocatalysis using immobilized titanium(IV) oxide nanoparticles, J. Photochem. Photobiol. A 182 (2006) 60–66.
[31] E. Vulliet, C. Emmelin, J.M. Chovelon, C. Guillard, J.M. Herrmann, Photocatalytic degradation of the herbicide cinosulfuron in aqueous TiO_2 suspension, Environ. Chem. Lett. 1 (2003) 62–67.
[32] H. Lachheb, E. Puzenat, A. Houas, M. Ksibi, E. Elaloui, C. Guillard, J.M. Herrmann, Photocatalytic degradation of various types of dyes (Alizarin S, Crocein Orange G, Methyl Red, Congo Red, Methylene Blue) in water by UV-irradiated titania, Appl. Catal. B 39 (2002) 75–90.
[33] A. Aleboyeh, H. Aleboyeh, Effects of gap size and UV dosage on decolorization of C.I. Acid Orange 7 by UV/H_2O_2 process, J. Hazard. Mater. B 133 (2006) 167–171.
[34] M. Stylidi, D.I. Kondarides, X.E. Verykios, Visible light-induced photocatalytic degradation of Acid Orange 7 in aqueous TiO_2 suspensions, Appl. Catal. B 47 (2004) 189–201.
[35] S. Bilgi, C. Demir, Identification of photooxidation degradation products of C.I. Reactive Orange 16 dye by gas chromatography–mass spectrometry, Dyes Pigments 66 (2005) 69–76.
[36] P. Calza, E. Pelizzetti, C. Minero, The fate of organic nitrogen in photocatalysis: an overview, J. Appl. Electrochem. 35 (2005) 665–673.
[37] C.S. Turchi, D.F. Ollis, Photocatalytic degradation of organic water contaminants: mechanisms involving hydroxyl radical attack, J. Catal. 122 (1990) 178–192.
[38] H. Al-Ekabi, N. Serpone, Kinetics studies in heterogeneous photocatalysis. I. Photocatalytic degradation of chlorinated phenols in aerated aqueous solutions over titania supported on a glass matrix, J. Phys. Chem. 92 (1988) 5726–5731.
[39] J. Beltran-Heredia, J. Torregrosa, J.R. Dominguez, J.A. Peres, Oxidation of *p*-hydroxybenzoic acid by UV radiation and by TiO_2/UV radiation: comparison and modelling of reaction kinetic, J. Hazard. Mater. B 83 (2001) 255–264.
[40] O. Levenspiel, Chemical Reaction Engineering, Wiley, NY, 1972.